Adsorption (2007) 13: 533–540
DOI 10.1007/s10450-007-9037-1

Characterization of gels via solvent desorption measurements

Cedric J. Gommes · Francis Noville · Jean-Paul Pirard

Received: 30 April 2007 / Revised: 23 July 2007 / Accepted: 24 July 2007 / Published online: 20 September 2007

Abstract The present paper shows how a standard volumetric adsorption device can be used to measure solvent desorption isotherms on gels. As gels are very soft materials, they shrink significantly during the measurement, and the data have to be analyzed in terms of the mechanical properties of the gel's skeleton. Methanol desorption isotherms are measured on a series of silica gels, and the results are compared with independent characterizations, notably beam bending.

Keywords Gels · Desorption · Drying · Plastic deformation · Capillary stress

1 Introduction

There are very few experimental techniques that can be used to characterize wet solids, and in particular gels. The application of most standard textural characterization techniques—such as microscopy, nitrogen adsorption and desorption, or mercury porosimetry (Lecloux et al. 1981; Kaneko 1994)—always requires the preliminary desiccation of the gel. The desiccation generally modifies greatly the structure of the gel so that, even if subcritical drying is used, there is no guarantee that the investigated solid is the same as the solid phase of the initial gel (Brinker and Scherer 1990). Examples of experimental techniques that can be used to characterize wet gels are Small-Angle X-Ray Scattering (SAXS) (Glatter and Kratky 1982; Kaneko 1994) and beam-bending (Scherer 1992).

C.J. Gommes (✉) · F. Noville · J.-P. Pirard
Department of Chemical Engineering, University of Liège,
Institut de Chimie B6a, Allée du 6 août 3, 4000 Liège, Belgium
e-mail: Cedric.gommes@ulg.ac.be

In the present paper, it is shown how a standard volumetric gas adsorption device can be used to measure solvent desorption from gels. Solvent desorption isotherms are often measured in the prospect of optimizing a drying process notably in the food industry, in which context the solvent is generally water (Mujumdar 1995). A common way to measure moisture content isotherms is to measure the mass loss of wet solid when put in equilibrium with various saline solutions. The present work is original in two respects. Firstly it proposes a new application of a class of commercially available devices. Secondly, it proposes a new method to characterize gels and in particular to analyze their mechanical properties for large deformations. The theoretical analysis of the data follows the same lines as those proposed by Reichenauer and Scherer (2000) to analyze nitrogen adsorption and desorption in compliant porous materials.

The outline of the paper is as follows. In the first section, the equivalence of desorption and drying is recalled, as well as a few theoretical expressions that are useful in the rest of the paper. The second section is experimental: the way in which the gels are synthesized, and how the sorptometer device is operated to obtain the solvent desorption curves, is explained. In the following section, the results are presented and the data are analyzed in terms of the plastic deformation of the gels' skeleton. Finally, the results are discussed in the light of previous characterization work performed on the same gels, notably by beam bending.

2 Theoretical backgrounds

A gel consists in two continuous phases (Fig. 1a): a liquid phase and a solid phase called the skeleton (Brinker and Scherer 1990; Osada and Gong 1998). The drying of a gel

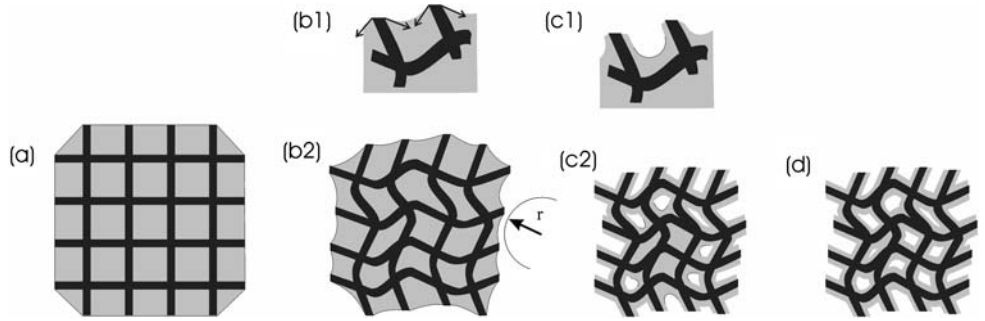

Fig. 1 A gel comprises a solid skeleton (in *black*) and a liquid phase (in *grey*) (**a**). When the liquid is being evaporated, menisci form at the gel's outer surface that put the skeleton in compression and the liquid in tension (**b1**): the gel shrinks (**b2**). When the radius of curvature of the menisci becomes comparable with the size of the pores of the shrunken skeleton (**c1**), the evaporation front enters in the gel's pores (**c2**). The desorption continues further by thinning of the adsorbed polymolecular solvent film (**d**)

and the desorption of a vapor out of a compliant material have the same phenomenology (Reichenauer and Scherer 2000). This is illustrated in Fig. 1, and it is discussed hereafter.

When the liquid phase is being evaporated, menisci form in the liquid at the gel's surface (Fig. 1b1), which puts the liquid phase in tension (Brinker and Scherer 1990). The negative pressure in the liquid is the capillary pressure P_c, which is related to the mean radius of curvature of the menisci r_m via the Young–Laplace Equation (de Gennes et al. 2004)

$$P_c = -\frac{2\gamma}{r_m} \tag{1}$$

where γ is the surface tension of the liquid. As a consequence of the tension in the liquid phase, the pressure P of the vapor in equilibrium with the liquid is lowered according the following general thermodynamic relation (Reichenauer and Scherer 2000)

$$P_c = \frac{RT}{V_m} \ln\left(\frac{P}{P_0}\right) \tag{2}$$

where R is the perfect gas constant, T is the absolute temperature, V_m is the molar volume of the liquid, and P_0 is the saturating pressure of the free liquid at the same temperature.

If the gel is saturated with liquid, then the compressive stress σ exerted on the skeleton is related to P_c by (Brinker and Scherer 1990)

$$\sigma = \left(1 - \frac{\rho}{\rho_s}\right) P_c \tag{3}$$

where ρ is the bulk density of the gel's porous skeleton, and ρ_s is the density of its dense backbone, so that the term between parenthesis is the volume fraction of liquid in the gel.

When the evaporation of the liquid proceeds, the compressive stress exerted on the skeleton increases, and the gel shrinks accordingly (Fig. 1b2). The shrinkage of the gel depends on the mechanical stiffness of the gel's skeleton. Provided the evaporation is slow compared to the time needed for the liquid to flow through the skeleton from the inside of the gel to its surface, P_c and σ are uniform through the gel. Under these circumstances, the gel's skeleton is a state of pure compression, with no shear. The only relevant mechanical parameter is the volume-dependent compression modulus $K(V) = V d\sigma/dV$, where V is the volume of the gel (Scherer et al. 1995).

The compression modulus of a gel during small deformations, K_0, can be measured via the beam bending of a gel rod (Scherer 1992). To the best of our knowledge, the compressive mechanical properties of a gel undergoing a large deformation have never been measured. It is, however, generally admitted that the mechanical properties of a gel and of the aerogel obtained by its supercritical drying are identical. When an aerogel is compressed to a volume larger than a given yield volume V_y its deformation is elastic and the compression modulus is constant at $K = K_0$. When the aerogel is compressed to a volume smaller than V_y, it undergoes a plastic deformation (Duffours et al. 1995) characterized by an increase of K according to (Scherer et al. 1995)

$$K = K_0 \left(\frac{V_y}{V}\right)^m \tag{4}$$

where m is an exponent that depends on the microstructure of the gel, and that generally obeys $3 < m < 4$, as notably reviewed by (Ma et al. 2000). In terms of volume-stress relation, the mentioned analytical forms of $K(V)$ imply (Scherer et al. 1995)

$$\sigma = K_0 \ln\left(\frac{V}{V_0}\right) \quad \text{for } V > V_y \tag{5}$$

and

$$\sigma = K_0 \ln\left(\frac{V_y}{V_0}\right) + \left(\frac{K_0}{m}\right)\left[1 - \left(\frac{V_y}{V}\right)^m\right] \quad \text{for } V < V_y \tag{6}$$

where V_0 is the volume of the relaxed gel's skeleton.

When the capillary stress has increased to such an extent that the mean radius of curvature of the menisci r_m has become comparable with the radius of the pores in the deformed skeleton, the contraction of the skeleton ceases (Fig. 1c1). Further drying of the gel occurs via the entering of the menisci inside the remaining porosity of the shrunken skeleton (Fig. 1c2). The vapor pressure at which the menisci start entering the gel's skeleton can be used to estimate the radius r of the pores in the shrunken skeleton, by combining (1) and (2), which leads to Kelvin's relation (Gregg and Sing 1982)

$$r = -\frac{2\gamma V_m}{RT\ln(P/P_0)} \tag{7}$$

in which the thickness of the polymolecular film of solvent adsorbed on the skeleton has been neglected, and the contact angle between the solvent and the skeleton was assumed to be 0.

3 Experimental sections

3.1 Synthesis of the gels

Gels are made from tetraethoxysilane (TEOS), 3-(2-aminoethylamino)propyl-trimethoxysilane (EDAS), H_2O, ethanol and NH_4OH via a single-step base-catalyzed hydrolysis and condensation, according to a protocol thoroughly described elsewhere (Gommes et al. 2006). The hydrolysis ratio $H = H_2O/(TEOS + 3/4\text{EDAS})$ is 4 for all gels, and the dilution ratio R = ethanol/(TEOS+EDAS) is 10. Five gels with EDAS/TEOS ratios = 0.025, 0.04, 0.1, 0.15 and 0.2 respectively are studied in the present paper; they are referred to hereafter as ET025, ET04, ET10, ET15 and ET20, respectively.

The gels were synthesized under the form of elongated cylinders about 2–3 cm long and 7.5 mm across, and they were aged in their mother liquor for one week at room temperature.

3.2 Solvent desorption measurements and data reduction

Prior to their measurements, the gels were washed several times in a large excess of methanol during at least two weeks, in order to replace their initial mother liquor with pure methanol. This particular choice of solvent is motivated by the fact that the vacuum grease and the silicon O-rings used in the sorptomatic device are poorly soluble in methanol.

A fraction of the gel cylinder is cut and placed in a glass tube for a desorption measurement on a standard volumetric device (Carlo Erba sorptomatic series 1990). The tube is placed in thermostatic bath at 20 °C.

As the commercial experimental device does not enable to perform a desorption run with no previous adsorption run, a bogus nitrogen adsorption is done first. The tube's tap is initially closed so that only the piston and piping are outgased and the gel's solvent does not start evaporating. Nitrogen is injected via the successive filling and emptying of the piston until the pressure reaches about 300 Torr (i.e about 40000 Pa), at which moment the tap is opened (see Fig. 2a). The value of 300 Torr was chosen because it is significantly larger than vapor pressure of methanol at 20 °C (about 95 Torr), and there is therefore no risk of boiling of the methanol when the pressure suddenly drops after the tap is opened.

The nitrogen injection proceeds afterwards with the tap open until a pressure about 600 Torr is reached. This bogus adsorption measurement with the tap open is used as a calibration step to estimate the free volumes of the device. Using the perfect gas law, the number of moles of nitrogen injected per piston is $\Delta N_i = P_l V_p / RT_p$, where P_l is the loading pressure, V_p and T_p are the volume and absolute temperature of the piston, and R is the perfect gas constant. In the same way, the pressure increase in the piping and in the tube subsequent to one injection is $\Delta P = (RT_c/V_c)\Delta N_i$, where the subscript c stands for chamber, which how the piping and the tube will be called hereafter. One has therefore $\Delta P = \alpha P_l$, with

$$\alpha = \frac{T_c V_p}{T_p V_c}. \tag{8}$$

As the loading pressure P_l is known precisely before each injection, and ΔP is also measured (see Fig. 2a), the adsorption run enables to estimate the numerical value of α, which is needed in the following.

When successive nitrogen injections have brought the pressure in the chamber at about 600 Torr, the device switches to the desorption mode. Successive pistons of gas are extracted, after each of which the pressure is let equilibrate until a given equilibrium criterion is met. The typical time for equilibrium is 10 min. Figure 2b plots the vapor pressures at which the system stabilizes after each volume extraction. The gas in the chamber is initially a mixture of air and of methanol vapor. During the first few extractions, the air initially present in the chamber is removed and replaced by the methanol that evaporates from the gel; the pressure decreases from the atmospheric pressure down to the vapor pressure of the saturated gel P_0 (see inset of Fig. 2b), at which moment no air is left in the chamber.

As the extraction proceeds, the gel dries progressively and the vapor pressure of methanol decreases. Let $P(n)$ be the partial pressure of the vapor in the chamber, after extraction n. When n is large, $P(n)$ is equal to the total pressure because there is no air left in the chamber. When n is small

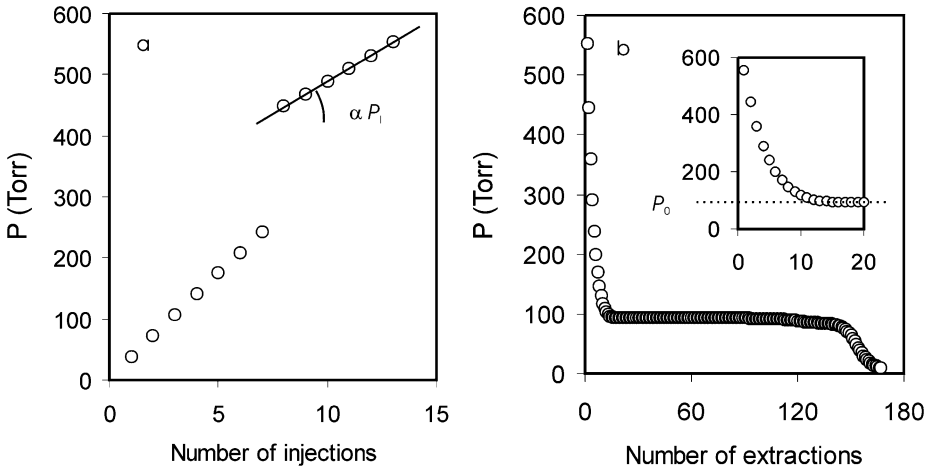

Fig. 2 Example of evolution of the pressure in the chamber following nitrogen injections (**a**) and subsequent vapor extraction (**b**). The jump in (**a**) corresponds to the opening of the tube's tap; the slope of the pressure increase is proportional to the piston loading pressure P_l. In (**b**), the pressure decreases rapidly when air is removed from the chamber until the saturation pressure P_0 is reached (*inset*). The following decrease of the pressure results from the progressive evaporation of the solvent

and air is still present in the chamber, one can confidently assume that $P(n) = P_0$, which corresponds to the horizontal dashed line in the inset of Fig. 2b.

At each extraction, the number of moles of solvent taken out of the chamber can be estimated using the perfect gas law as $(V_p/RT_p)P(n)$, with the same notations as in (8).

The solvent is present in the chamber under the form of a liquid filling the gel's porosity as well as and under the form of a vapor, the number of moles of which is estimated as $(V_c/RT_c)P(n)$, where the subscript c stands for chamber. Therefore, the number of moles of solvent evaporated from the gel $\Delta N_{\text{evap}}(n)$ during the n^{th} extraction can be estimated as

$$\Delta N_{\text{evap}}(n) = \frac{V_p}{RT_p}P(n) - \frac{V_c}{RT_c}[P(n) - P(n-1)] \qquad (9)$$

where the first term is the total number of moles of vapor extracted, and the second term is the correction due to the change of number of moles of vapor in the chamber. Using (8), (9) can be written more conveniently as

$$\Delta N_{\text{evap}}(n) = \frac{V_p}{RT_p}\left(P(n) - \frac{1}{\alpha}[P(n) - P(n-1)]\right). \qquad (10)$$

Every constant in (10) is known: the volume of the piston is calibrated ($V_p = 17.041$ cm^3 in the used device), the temperature in the piston is also controlled ($T_p = 37\,^\circ$C), and α is known from the adsorption run (see the discussion leading to (8), and Fig. 2a).

Using (10) iteratively, the number of moles of solvent in the gel $N(n)$ at any stage of the drying can be estimated. In particular, by summing all the values of $\Delta N_{\text{evap}}(n)$, the total amount of solvent evaporated from the gel during the measurement is estimated. In Fig. 3, this estimation is compared with the difference in weight of the sample before and after the measurement. The mass loss estimated from (10) is always a few percent smaller than the weighed mass loss; the agreement is nevertheless very good.

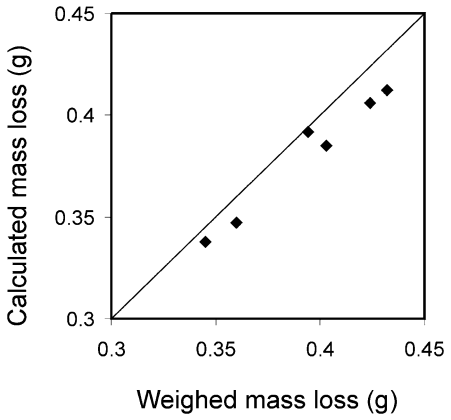

Fig. 3 Comparison of the gel's mass loss calculated from the desorption measurement with (10), with the difference of mass weighed before and after the runs

4 Results

Figure 4a plots the solvent desorption curves of the gels. Close to the saturation, all curves start from a vapor pressure between 93.8 and 94.5 Torr, which is slightly smaller than the vapor pressure of pure methanol measured in the same conditions on the same device (95.6 Torr). The curves exhibit a vertical asymptote and they bend upwards when the pressure is lowered. A bend is observed at intermediate pressure, as indicated by an arrow in Fig. 4a, with a quasi-riser in the curves. At still lower pressure, the solvent content decreases almost linearly until the gels are completely dry. The bend corresponds to the critical point of drying (Fig. 1c1): at larger pressure the gel is compressed by the menisci that form at the gel's surface, at smaller pressure the porosity empties from methanol.

Figure 4b analyzes the large pressure part of the desorption curves in terms of the mechanical properties of the gels. For that purpose, (2) and (3) are used to estimate the compressive stress σ corresponding to a partial pressure P/P_0,

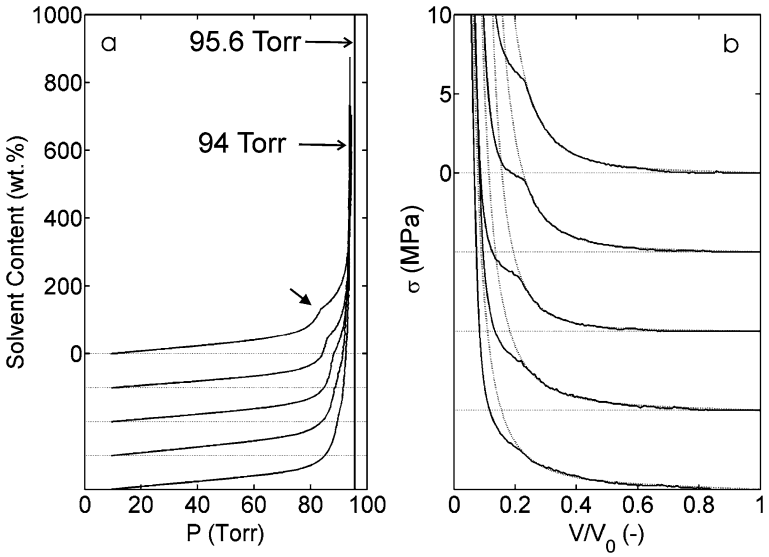

Fig. 4 Methanol desorption curves measured on the gels (**a**), in which the arrow indicates the critical point of drying. The same experimental data are expressed in (**b**) under the form of compression curves of the gel's skeleton, where (2) and (3) were used to convert P to σ. The *vertical line* in (**a**) is the vapor pressure of free methanol; the *dotted lines* in (**b**) are least square fits of the data with (5) and (6). The curves are shifted vertically, with gels ET025, ET04, ET10, ET15 and ET20 from bottom to top

with P_0 estimated from the position of the vertical asymptote in each desorption curve (Fig. 4a). The volume of the gel was estimated by assuming that any solvent loss results from a macroscopic shrinkage of the gel, and the volumes were normalized by the initial volume of the gels. The initial volume of the gels V_0 was estimated as the sum of the volume of the skeleton's backbone and of the liquid as

$$V_0 = \frac{m_d}{\rho_s} + \frac{m_w - m_d}{\rho_l} \tag{11}$$

where m_w and m_d are the masses of the wet and dry gels, respectively, measured before and after the run, and ρ_s and ρ_l are the densities of the skeleton's backbone and of the liquid. The used values are $\rho_s = 2$ g/cm^3 (Gommes et al. 2006), and $\rho_l = 0.792$ g/cm^3 for methanol (Weast and Astle 1982). It has to be kept in mind that the analysis of the data in terms of compression of the skeleton is valid only as long as the gel remains saturated (Fig. 1b2); the curves in Fig. 4b are meaningless for values of V/V_0 lower than the bend.

The diameter of the gel cylinders is measured after the end of the measurement, and the linear shrinkage are found to be between $L/L_0 = 0.56$ and 0.62, which corresponds to volume shrinkage $V/V_0 = (L/L_0)^3$ between 0.18 and 0.24. These numbers are in good agreement with the position of the bend in Fig. 4b, which confirms the qualitative interpretation of the curves in Figs. 4a and b in terms of shrinking and subsequent drying of the shrunken gel.

The experimental curves of σ versus V/V_0 were fitted with (5) and (6), with K_0 and m as adjustable parameters. The yield volume V_y was assumed to be $V_y = V_0 \exp(-1/m)$, which relation has been proposed by other authors based on experimental observation on many silica aerogels (Smith et al. 1995). As is visible on Fig. 4b, the model fits very satisfactorily the curves; the adjusted values of K_0 and of m are reported in Table 1. When V_y, K_0, and m are all used as adjustable parameters, the best fit is always obtained with $V_y = V_0$. As reported in Table 1, this leads to smaller values of K_0, but the values found for m are globally close to those obtained by assuming $V_y = V_0 \exp(-1/m)$.

Table 1 Characteristics of the gels determined from solvent desorption and from other methods

	K_0 (MPa)	m (−)	r (nm)	K_g[a] (MPa)	m_a[a] (−)	L_w[a] (nm)
ET025	0.67 (0.39)	2.0 (1.6)	16.0	0.11	4.9	701
ET04	0.62 (0.33)	2.3 (2.0)	14.0	0.20	4.0	479
ET10	0.22 (0.10)	3.2 (3.1)	11.2	0.55	3.4	161
ET15	0.44 (0.19)	3.1 (2.9)	8.8	0.65	3.6	121
ET20	0.55 (0.25)	3.1 (2.9)	6.8	1.22	3.0	79

K_0 and m: Elastic compression modulus and plastic hardening exponent of the gels determined from methanol desorption. The numbers between parentheses were obtained with K_0, m and V_y as fitting parameters, in which case the best fit is always found for $V_y = V_0$; r: radius of the meniscus at the critical point of drying; K_g: elastic modulus of the gel determined by beam bending; m_a: plastic hardening exponent of the aerogel, determined by mercury porosimetry; L_w: pore size in the gels, determined by beam bending

[a]Taken from Gommes et al. (2007, submitted)

From the vapor pressure at which the menisci start entering the gel's porosity, the pore size can be estimated via Kelvin's relation. Using the values $V_m = 40.46$ ml/mol and $\gamma = 22.6 \times 10^{-3}$ N/m, valid for methanol at 20 °C (Weast and Astle 1982), (7) becomes

$$\ln\left(\frac{P}{P_0}\right) = -\frac{0.75}{r} \tag{12}$$

if the radius of the meniscus r is expressed in nm. The position of the bend in the desorption curves was the determined manually as the point where (5) and (6) are no longer able

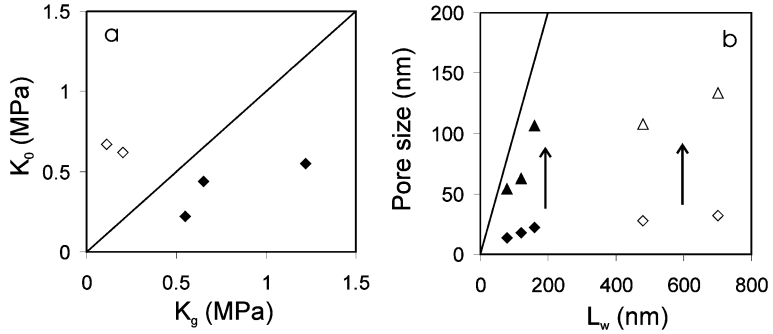

Fig. 5 (**a**) Comparison of K_0 with the compression modulus K_g estimated by beam bending. (**b**) Comparison of pore size estimated by methanol desorption with pore size estimated by beam bending L_w. *Lozenges* are for the shrunken gel, and the *triangles* are corrected for the shrinkage of the gels; the correction is symbolized by the *arrows*. In both graphs, the *open symbols* are for gels ET025 and ET04, and the *solid line* is the identity line $y = x$

to fit the data, and the corresponding radius is reported in Table 1.

5 Discussion

5.1 Comparison with other techniques

Table 1 compares the values of K_0, m and r estimated from the methanol desorption curves, with independent estimates made on the same gels and to be published elsewhere (Gommes et al. 2007, submitted): K_g was measured by beam bending, m_a was measured by drying the gel in supercritical conditions and by compressing the obtained aerogel in a mercury porosimeter, and L_w is an estimate of the pore size of the gel, also obtained from the bending measurements.

At first sight, the gels ET025 and ET04 seem to be outliers. When passing from ET20 to ET025, K_g decreases and m_a increases continuously; the same evolution is seen for K_0 and m for gels ET20 to ET10, but the evolution is opposite for the two other gels (see also Fig. 5a). The values of m obtained for ET10 to ET20 are between 3 and 4, which compares well with values typical of a large variety of silica aerogels (Ma et al. 2000). On the other hand, the values of m for ET025 and ET04 are close to 2, which value is generally encountered for cellular materials (Gibson and Ashby 1988).

In order to use r and (12) to estimate the size of the pores in the gel, a correction has to be made to account for the shrinkage of the gels during desorption. There is experimental evidence that during the compaction of a gel the size of the pores shrink proportionally to the pore volume, rather than to the third root (Smith et al. 1995). A reasonable estimate of the pore diameter would therefore be

$$L_{\text{pore}} = 2r\frac{V_0}{V} \tag{13}$$

where it has been assumed that the dilution is such that the volume of the gel is a good estimate of its pore volume. As visible in Fig. 5b, the estimates of the pore size based on (13) are in good agreement with the pore size measured by beam bending for gels ET20, ET15 and ET10. Once again ET025 and ET04 are outliers, as their pore size seems to be strongly underestimated by the present technique.

The differences between K_0 and K_g for ET10, ET15 and ET20 that are visible in Fig. 5a, do not necessarily mean that the mechanical characterizations of the gels are inaccurate *in the measured deformation range*. It has to be kept in mind that the present measurements of methanol desorption imply a large deformation of the gels, with typical linear strain of $L/L_0 = 0.6$ as mentioned previously, while the maximum linear strain in the beam bending measurements is about $L/L_0 = 0.02$ (Gommes et al. 2007, submitted). In principle, the elastic modulus K_0 could be obtained from the analysis of the $\sigma(V/V_0)$ curves in the elastic deformation range, on the basis of (5). In practice, however, a significant shrinkage of the gels occurs at compressive stresses that are too low to be measured by the proposed technique (Fig. 4b). The stresses become large enough to be measured only for $V/V_0 < 0.8$, i.e. in the plastic deformation range.

In the present paper, the mechanical characterization is therefore mainly done in the plastic region, and K_0 is merely an extrapolation of the measurement to the region of small deformations that is inaccessible via the present experimental technique. The extrapolation is based on (5) and (6) that do not necessarily apply. For instance, some gels exhibit a lowering of their compression modulus at the beginning of their compression (Gross et al. 1992; Gommes et al. 2005; Chaudhuri et al. 2007). This might be the reason why K_0 underestimates K_g for gels ET10 to ET20. The fact that the exponent m is reasonably close to m_a, also measured by large deformation of the aerogels, suggests that the plastic characteristics of the gels be estimated with a reasonable accuracy.

5.2 Validity of the method and accuracy

The various results presented in the previous sections are based on various assumptions of different nature. The conditions of validity of these results are therefore not the same. On one hand, the analysis leading to the $\sigma(V)$ curves relies only on a general thermodynamic relation (2) and on a general force balance relation (3). Both relations hold in the simple hypothesis that the liquor filling the pores of the gel is a pure liquid. As the gels were washed several times, over long periods, in large excess of methanol, there are good reasons to believe that the hypothesis is satisfied. On the other hand, data on pore size is subject to hypotheses about the pore shape, thickness of the polymolecular adsorbed film, contact angle (7), as well as on the stretching of the pores during drying (13). Therefore, the pore size obtained by combining (12) and (13) has to be considered as an order of magnitude.

Let us now estimate the experimental error on both V and σ. From Fig. 3, one sees that the error on the total mass of evaporated liquid estimated through the repeated use of (10) is about 5%, when compared to the weighed mass loss of the sample during the run. As the volume reduction of the gel during the first stage of drying is proportional to its mass loss, the relative error on the volume reduction of the gel is also 5%. Concerning the uncertainty on σ, it mostly results from the poor knowledge of P_0. Based on the observed scatter in P_0 for the various gels (see Sect. 4), one can estimate the uncertainty on P_0 to be about 1 Torr. From (2), it is found that this uncertainty on P_0 leads to an uncertainty of about 0.6 MPa on P_C. From (3) and since the relative uncertainty on ρ is the same as on V, one finds that the uncertainty on σ is also about 0.6 MPa, i.e. about 10% of the maximum stress for ET20 and 20% for ET025 (see Fig. 4b).

6 Conclusions

The present paper demonstrates the feasibility of measuring mechanical properties of gels in their plastic deformation range using a standard volumetric device available commercially and intended for measuring gas adsorption and desorption isotherms. A bogus nitrogen adsorption run is first performed that enables to estimate the free volume of the device. During the subsequent desorption run, the pressure at which the system stabilizes after each gas extraction is exported, from which the methanol desorption isotherms are measured.

The solvent desorption of a gel is equivalent to its drying. During the first stage of drying the gel shrinks and it remains saturated; using very general thermodynamic and mechanic relations, the corresponding part of the desorption curve can be analyzed quantitatively in terms of the stress-volume relation of the gel's skeleton. The second stage of drying begins when the drying front penetrates the gel's porosity; making assumptions on the pore stretching and emptying processes, the pressure at which this occurs can be related to the size of the pores in the gel.

The characteristics of the gels, in terms of pore size and compression modulus, for the present technique to be accurate still have to be investigated in a systematic way. However, the error on gel volume is likely to be lower than about 5% and the error on the compressive stress is estimated to be about 0.6 MPa. In the present study, a reasonable agreement with independent experimental techniques was obtained for gels with $K_0 > 0.22$ MPa and pores smaller than 160 nm.

Acknowledgements C.J.G. is a postdoctoral researcher of the Belgian National Fund for Scientific Research (FNRS). The authors are grateful to Professor George W. Scherer for reading and commenting the first draft of the manuscript. This work was supported by the National Funds for Scientific Research, Belgium, and by the Région Wallonne—Direction Générale des Technologies de la Recherche et de l'Énergie.

References

Brinker, C.J., Scherer, G.W.: Sol–Gel Science: The Physics and Chemistry of Sol–Gel Processing. Academic Press, San Diego (1990)
Chaudhuri, O., Parekh, S.H., Fletcher, D.A.: Reversible stress softening of actin networks. Nature **445**, 295–298 (2007)
de Gennes, P.-G., Brochard-Wyart, F., Quéré, D.: Capillarity and Wetting Phenomena: Drops, Bubbles, Pearls, Waves. Springer, New York (2004)
Duffours, L., Woignier, T., Phalippou, J.: Pastic behaviour of aerogels under isostatic pressure. J. Non-Cryst. Solids **186**, 321–327 (1995)
Gibson, L.J., Ashby, M.F.: Cellular Solids, Structure and Properties. Pergamon, Oxford (1988)
Glatter, O., Kratky, O.: Small Angle X Ray Scattering. Academic, New York (1982)
Gommes, C.J., Job, N., Blacher, S., Pirard, J.-P.: Compressing some sol-gel materials reduces their stiffness: a textural analysis. Stud. Surf. Sci. Catal. **160**, 193–200 (2005)
Gommes, C.J., Basiura, M., Goderis, B., Pirard, J.-P., Blacher, S.: Structure of silica xerogels synthesized with organoalkoxysilane co-reactants hints at multiple phase separation. J. Phys. Chem. B **110**, 7757–7765 (2006)
Gommes, C.J., Blacher, S., Pirard, J.-P., Scherer, G.W.: The microstructure of hybrid silica gels and its modification by evaporative and supercritical dryings. J. Sol–Gel Sci. Technol. (2007, submitted)
Gregg, S.J., Sing, K.S.W.: Adsorption, Surface Area and Porosity. Academic Press, London (1982)
Gross, J., Fricke, J., Pekala, R.W., Hrubesh, L.W.: Elastic nonlinearity of aerogels. Phys. Rev. B **45**, 12774–12777 (1992)
Kaneko, K.: Determination of ore size and pore size distributions: 1. Adsorbent and catalysts. J. Membr. Sci. **96**, 58–89 (1994)
Lecloux, A.J.: Texture of catalysts. In: Anderson, J.R., Boudart, M. (eds.) Catalysis: Science and Technology, vol. 2, pp. 171–230. Springer, Berlin (1981)
Ma, H.-S., Roberts, A.P., Prévost, J.-H., Jullien, R., Scherer, G.W.: Mechanical structure-property relationship of aerogels. J. Non-Cryst. Solids **277**, 127–141 (2000)
Mujumdar, A.S.: Handbook of Industrial Drying, 2nd edn. Dekker, New York (1995)

Osada, Y., Gong, J.-P.: Soft and wet materials: polymer gels. Adv. Mater. **10**, 827–837 (1998)

Reichenauer, G., Scherer, G.W.: Nitrogen adsorption in compliant materials. J. Non-Cryst. Solids **277**, 162–172 (2000)

Scherer, G.W.: Bending of gel beams: method for characterizing elastic properties and permeability. J. Non-Cryst. Solids **142**, 18–35 (1992)

Scherer, G.W., Smith, D.M., Qiu, X., Anderson, J.M.: Compression of aerogels. J. Non-Cryst. Solids **186**, 316–320 (1995)

Smith, D.M., Scherer, G.W., Anderson, J.M.: Shrinkage during drying of silica gel. J. Non-Cryst. Solids **188**, 191–206 (1995)

Weast, R.C., Astle, M.J. (eds.): CRC Handbook of Physics and Chemistry, 63rd edn. CRC Press, Boca Raton (1982)